Pedestrian trajectory prediction based on improved avoidance force algorithm

Tao Peng [1], Yalong Kang [2], Junping Liu [1], Feng Yu [1], Xinrong Hu [1], Ruhan He [1], and Minghua Jiang [1]

[1]Affiliation not available
[2]Wuhan Textile University

October 30, 2023

Abstract

The complexity of interactions between pedestrians poses a challenge to pedestrian trajectory prediction, and existing trajectory prediction methods based on data-driven models lack interpretation for modeling interactions between pedestrians. To address this problem, an improved avoidance force algorithm is proposed to model the interaction of pedestrian forces explicitly. Multiple socially acceptable pedestrian trajectory information is generated by using the prior knowledge of observed trajectory and the avoidance force algorithm.The avoidance force trajectories are evaluated by an attention network to generate confidence scores; the avoidance force trajectories are selected based on the confidence scores;The final accurate trajectories are refined using Teacher-forcing. Compared to Social-Implicit, ours experimental results conducted on the ETH and UCY datasets show that the proposed method improves the average displacement error (ADE) and final displacement error (FDE) by 6\% and 16\%, respectively.

Pedestrian trajectory prediction based on improved avoidance force algorithm

Tao Peng, Yalong Kang, Junping Liu, Feng Yu, Xinrong Hu, Ruhan He, Minghua Jiang

***Abstract*—The complexity of interactions between pedestrians poses a challenge to pedestrian trajectory prediction, and existing trajectory prediction methods based on data-driven models lack interpretation for modeling interactions between pedestrians. To address this problem, an improved avoidance force algorithm is proposed to model the interaction of pedestrian forces explicitly. Multiple socially acceptable pedestrian trajectory information is generated by using the prior knowledge of observed trajectory and the avoidance force algorithm.The avoidance force trajectories are evaluated by an attention network to generate confidence scores; the avoidance force trajectories are selected based on the confidence scores;The final accurate trajectories are refined using Teacher-forcing. Compared to Social-Implicit, ours experimental results conducted on the ETH and UCY datasets show that the proposed method improves the average displacement error (ADE) and final displacement error (FDE) by 6% and 16%, respectively.**

***Index Terms*—Social force, Avoidance algorithm, Self-attention, Teacher-forcing.**

I. Introduction

THE workflow of pedestrian trajectory prediction is to predict the trajectory information of one or more interacting bodies in the future given the prior knowledge of the known observation trajectory. As an important component of unmanned vehicles, intelligent transportation, and interactive robots, pedestrian trajectory prediction has become a hot research direction[1].

Much of the early work was based on data-driven[2] approaches, which are better at fitting data and can learn from a large number of datasets. They do, however, lack a certain level of interpretability.The next approach is based on physical rules, which are derived from certain knowledge of physics and have good interpretability.

However, the physical rule-based approach is less efficient than the data-driven approach in terms of data fitting due to the inherent physical rule constraint. Therefore, a pedestrian force model incorporating neural networks is proposed in this paper. The technical route of this paper consists of two major parts: 1) generating multiple socially acceptable trajectory information by improving the avoidance force algorithm model; 2) evaluating the avoidance force trajectories by attention networks to generate confidence scores; and selecting the avoidance force trajectories based on the confidence scores.

Manuscript created October, 2020; This work is partly supported by the Cixi Science and Technology Bureau under Grant No.2021Z069 and Department of Education of the Hubei Province of China under Grant No.D20211701, and the Engineering Research Cen ter of Hubei Province for Clothing Information.

The authors extend their appreciation to the Department of Education of the Hubei Province of China for fund ing this research work through grant No.2020BAB116 and No.D20211701. The help of Hubei Provincial Engineering Research Center for Intelligent Textile and Fashion and En gineering Research Center of Hubei Province for Clothing Information in this research completion is greatly appreciated.

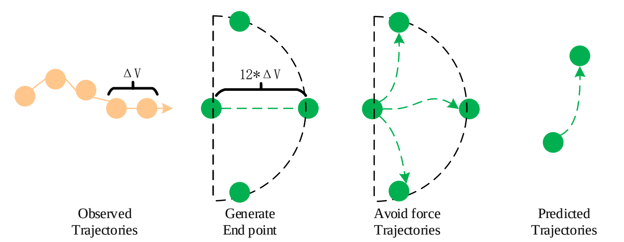

Fig. 1. The framework of overview.Given the observed trajectories of pedestrians, generate endpoints. Use the initial endpoint to sample all endpoint information, then complete the complete trajectory by improving the avoidance force, and finally select the best trajectory.

The steps of generating an improved collision avoidance force trajectory conforming to pedestrian movement characteristics are mainly divided into two parts: 1) the generation of pedestrian trajectory endpoints; 2) the generation of complete improved avoidance force trajectories using the improved avoidance force algorithm based on the trajectory endpoint information. As shown in Figure 1, in order to express the generation of trajectory endpoints more concisely, the future trajectory is generated using the higher-order velocities of the last two frames of the observed trajectory, and the obtained trajectory is the trajectory in the straight-ahead direction.Using the observed end point as the center of the circle and the straight trajectory as the radius, the trajectory is uniformly rotated at a certain angle in order to obtain all the end point sampling information.

In order to generate the complete improved avoidance force trajectory, the improved avoidance force is used to complement the complete trajectory information. The social force model, as a basic model for describing pedestrian motion, can simulate pedestrian motion in the normal state. However, the selection of avoidance for two-way pedestrian flow is still a difficult area of current research, where pedestrians will traverse each other in the case of zero longitudinal distance. Current research on the avoidance problem has focused on deceleration avoidance [3] and proposes active avoidance forces [4] as well as changing the desired direction for selective avoidance.

The avoidance algorithm proposed in this paper is based on the tradition active avoidance force for decision optimization, and the research focuses on the following: for two-way pedestrian flow(A pedestrian walking in opposite directions), not only pedestrians with zero longitudinal distance will choose

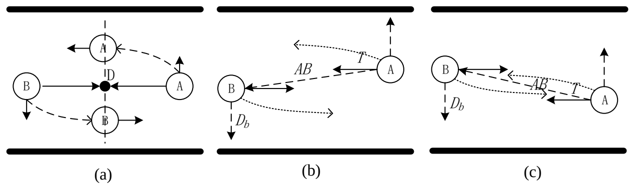

Fig. 2. Avoidance Strategies. The active avoidance force is indicated by (a); (b) indicates that the active avoidance force can be used to avoid normally; and (c) indicates that the pedestrian will traversing the horizontal center line to perform abnormal avoidance using the active avoidance force.

to avoid; for opposite pedestrians with a longitudinal distance less than the sum of the radius of two lines of people in the vertical direction, such pedestrians will still choose to avoid as well.Tradition active avoidance force-based avoidance algorithm In this case, there is distortion. The specific distortion problem is shown in the following two aspects:1)tradition active avoidance force principle is the pedestrian to the right to change their own direction of motion, this algorithm has certain limitations, as shown in Figure 2, pedestrian (a), (b) can simulate the normal avoidance mode, if A, B position changes as shown in (c), tradition active avoidance force algorithm in this In this case, there is a distortion situation:A, B will not choose the direction of collision avoidance nearby, but chooses a far collision avoidance path, which is not in line with the actual situation. To address this problem, this paper proposes a dynamic direction decision avoidance algorithm, which can dynamically change the avoidance direction according to the relative position of the pedestrian, so that the trajectory prediction results are closer to the real situation. 2) In the tradition active avoidance force algorithm, in the process of choosing avoidance, entities A and B will deflect to avoid. However, in the actual situation, it is more likely that pedestrians on one side will avoid, and pedestrians on the other side will go straight ahead, so the tradition active avoidance force algorithm has this defect in the simulation of the avoidance process.To address this problem, this paper proposes a dynamic selection avoidance algorithm, which selects whether to avoid or not by calculating the relative values of the velocity mapping of entities A and B on vectors AB and BA, so that the trajectory prediction can be closer to the real two-way pedestrian flow.

In order to select the optimal path from the multiple improved avoidance force trajectory, the improved avoidance force trajectory is evaluated by the attention network to generate a confidence score; The improved avoidance force trajectory is selected as the initial prediction trajectory based on the confidence score. The ground truth trajectory is used to generate the ground truth coarse trajectory, and the generated ground truth coarse trajectory is used to optimize the trajectory closest to it in the initial prediction trajectory. In the training phase, the top-1 trajectory is selected as the preliminary prediction trajectory, and then refined for refinement using Teacher-forcing[5]; In the inference phase, the top-k preliminary prediction trajectory is selected to serve as the final prediction trajectory. The contributions of this paper are as follows: 1) An improved avoidance force algorithm is proposed to describe the avoidance pattern among pedestrians. 2)The improved collision avoidance algorithm is used to generate the pedestrian trajectory that conforms to the characteristics of pedestrian movement. 3) The generated trajectory of improved avoidance force can explicitly interpret the trajectory information of pedestrian's future movement.

II. Related Work

A. *Pedestrian trajectory prediction*

Pedestrian trajectory prediction in the early days adopted a deterministic rule-based approach using models such as social forces [6], Bayesian filters and kinematic model combinations [7], Markov processes [8], and dynamic Bayesian networks [7]. Relying on prior knowledge, the manual method explicitly expresses the interpretability of trajectory prediction. These trajectory prediction methods require rigorous modeling of the model and have limitations that make them difficult to generalize to complex scenarios.

In recent years, data-driven approaches based on image recognition [9], [10], [11], behavior recognition [12], and visual localization [13] have made remarkable progress. Since no inherent rule models need to be pre-defined, better mapping relationships can be fitted by virtue of large-scale datasets. Similarly, data-driven-based approaches have led to significant progress in pedestrian trajectory prediction. A large number of data-driven trajectory prediction methods have been proposed, Alahi [2] et al. used the Social Long Short-Term Memory (S-LSTM) network to extract interactions between nearby pedestrians and set up a social pool to share information about interactions between pedestrians. sophie [14] used CNN to extract features from the whole GAT. Social-BIGAT [15] uses LSTM to model the trajectory of each pedestrian and the interaction of the Graph Attention network (GAT). STAR [16] models spatial interactions and temporal dependencies through the Transformer framework. SGCN [17] proposes a sparse graph convolutional network that models spatial and temporal graphs separately to learn pedestrian interactions and pedestrian movement trends to predict pedestrian trajectories. SGAN [18] uses a Generative Adversarial Network (GAN) to model pedestrian trajectories. Social-STGCNN [19] directly models the pedestrian trajectory as a graph, where the edges are weighted by the relative distance between pedestrians to represent the interaction between pedestrians. Social-Implicit [20] constructs a Social-Zone, which aggregates the observed trajectories based on the observed maximum velocity. Each Social-Zone is then processed by a Social-Cell, which consists of a local stream and a global stream, each consisting of two CNNs.

B. *Social force model*

The social force model consists of three major components: self-driven forces of pedestrians; interaction forces between pedestrians; and interaction forces between pedestrians and obstacles. The self-driven force between pedestrians is in accordance with Newton's second law, which indicates that pedestrian sets out at the desired speed towards the desired destination; The interaction force between pedestrians includes psychological repulsive force and physical contact force. The psychological repulsive force is the force manifested by the fact that pedestrians automatically maintain a certain distance with other pedestrians during the walking process. Physical contact force refers to the physical positive pressure and sliding friction generated when pedestrians are very close to each other. The forces between pedestrians and obstacles are described as physical contact forces and psychological repulsion forces between pedestrians and obstacles.

C. Active avoidance force

The active avoidance force [4] is a judgment mechanism based on the valid conflict point, and after the conflict point is determined to be valid, the pedestrian's right avoidance is used as the benchmark to choose avoidance, as shown in Figure 3.

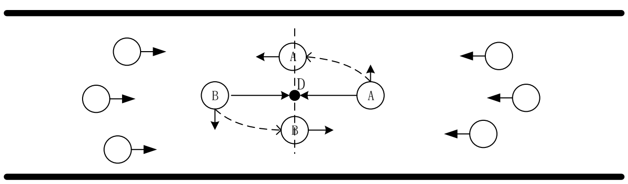

Fig. 3. Tradition active avoidance force. Pedestrians will choose to avoid to the right.

The tradition active avoidance force is related to the target direction of pedestrians and the density of pedestrians, which are defined in equation (1).

$$F_a = A \cdot exp(D/B) \cdot \cos\alpha \cdot d_j \tag{1}$$

where A denotes the force intensity coefficient of the pedestrian, D denotes the distance between the pedestrian's new destination and the potential conflict point, B denotes the range of the pedestrian's force, $\cos\alpha$ denotes the cosine of the angle between the vector of the pedestrian pointing to the new destination and the current velocity; and d_j denotes the unit vector perpendicular to the desired direction.

III. Improved avoidance force trajectory

Existing works has used deep learning networks to construct pedestrian interactions, Graph convolutional networks with physical adjacency matrices [21] and attention mechanisms with learnable adjacency matrices [22] have been used to inherit spatial interaction information. This approach is able to de-learn features from a large amount of data, but still lacks some interpretability for constructing pedestrian forces.In order to explicitly construct the force between pedestrians, a pedestrian trajectory prediction based on improved avoidance force trajectory is proposed.The general framework is shown in Figure 7. Firstly, the endpoint information of the pedestrian trajectory is generated using the observed trajectory, and the complete trajectory information is complemented by the improved avoidance force. Then, the generated improved avoidance force trajectories are embedded and encoded, while the spatial interactions of the observed trajectories are encoded, and by attention, each trajectory is scored, and the trajectories with high confidence are selected and optimized. Finally, the trajectories are further optimized using Teacher-forcing in the training process.

A. Improved avoidance force trajectory

In order to generate rough trajectory endpoint information for pedestrians, first the higher-order velocity of the last two frames of the observed trajectory is used as a way to advance the future trajectory and thus to obtain the trajectory information in the straight ahead direction. Assuming the prediction length $T_{pred} = T_{all} - T_{obs} = 12$, a straight trajectory with a depth of $d = 12$ will be generated. After obtaining the initial straight trajectory, take the end point of the observed trajectory as the center of the circle and the initial straight trajectory as the radius, and rotate the sampling to the left and right sides at a certain angle $\theta(\theta+ <= \pi/2)$ to obtain all the end point sampling information.

In order to generate the complete trajectory information of the improved avoidance force, the improved avoidance force is adopted, In order to avoid the collision of pedestrians coming in the opposite direction, that is, the direction of the line of the center of gravity of pedestrians coincides with the direction of the resultant force of pedestrians (as shown in Figure 2 (a)), it is necessary to introduce the active avoidance force to avoid collision with each other, so as to solve the phenomenon of pedestrians crossing each other in the primitive social force. With the increase of pedestrian density, the phenomenon of pedestrians crossing each other will become more serious. However, the tradition active avoidance force has certain defects in design, and this paper introduces a dynamic direction decision avoidance algorithm and a dynamic selection avoidance algorithm for the original active avoidance force to solve the defects of the tradition active avoidance force.

1) Dynamic directional decision avoidance algorithm: The tradition active avoidance force only considers the special case where the direction of the pedestrian's center of gravity(in Figure 2 (a)) and the direction of the pedestrian's combined force coincide, and the design is based on avoidance to the right. Considering that for two-way pedestrian flow, not only the pedestrians whose center of gravity line direction coincides with the direction of pedestrian occur avoid, but also the opposing pedestrian flow whose longitudinal distance of the center of gravity is less than the sum of the radii of the two pedestrians occur avoid. As the traditional active avoidance force adopts the right avoidance strategy, it will lead to pedestrians not choosing to avoid nearby: as shown in Figure 4, the positions of pedestrians A and B are as shown in the figure.If according to the traditional active avoidance force, when the opposite pedestrians are found, A and B will make the right avoidance strategy, and then both sides of pedestrians will cross the horizontal centerline to avoid, rather than choose to avoid in the nearest direction, which is inconsistent with the actual situation.

To address the above problem, this paper proposes a dynamic directional decision avoidance algorithm, which can

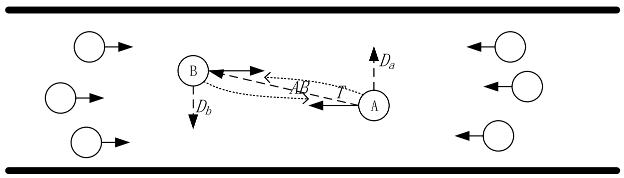

Fig. 4. Abnormal avoidance. Using the principle of active avoidance force, pedestrians will traverse the horizontal center line for abnormal avoidance.

select the avoidance direction according to the relative position of the pedestrian in close proximity, rather than just choosing the avoidance direction to the right. The choice of avoidance direction is actually the choice of vertical vector, as shown in Figure 5, assuming that T vector is the unit vector of pedestrian A pointing to the target position, D_a and D_a' are the unit vectors perpendicular to it, vector AB is the unit vector of A pointing to B, $\cos\langle AB, D_a\rangle$ and $\cos\langle AB, D_a'\rangle$ are the cosines of AB and the perpendicular vector, respectively. The choice of the vertical vector is defined in equation (2).

$$D_a = g\left(\cos\left(AB, D_a\right) \leq 0?D_a : D_a'\right) \tag{2}$$

The $g\{\cdot\}$ function indicates that if the equation holds, the D_a is returned, and if it does not hold, the D_a' is returned. The avoidance direction of the pedestrian is determined by calculating the corresponding cosine value, and a cosine value less than zero indicates that the corresponding vertical vector is the vertical vector in the direction of proximity avoidance, and vice versa.

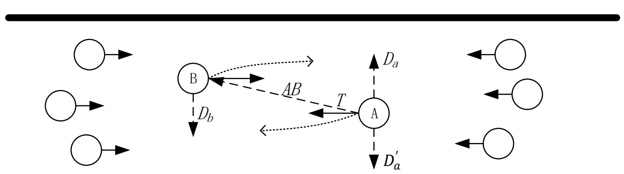

Fig. 5. Dynamic direction decision avoidance. Pedestrians will choose to avoid them according to their relative positions.

Since the improved collision avoidance force is optimized based on the traditional active collision avoidance force, after determining the pedestrian collision avoidance direction, the improved collision avoidance force can be understood as the active collision avoidance force that can automatically select the collision avoidance direction, so the improved collision avoidance force is defined as: (3).

$$F_{imp} = A \cdot exp(D/B) \cdot \cos\alpha \cdot D_a \tag{3}$$

F_{imp} is the avoidance force after improving the decision direction; D is the distance between the pedestrian's new destination and the potential conflict point; α is the angle between the vector of pedestrian A pointing to B and the velocity direction of the current entity A; and D_a is the unit vector dynamically chosen to be perpendicular to the desired direction.

2) Dynamic selection avoidance algorithm: In the design of the Active avoidance principle, the two entities that are about to be avoided are equal entities. That is, in the occurrence of avoidance, both entities will choose to avoid. While the principle of avoidance in the real world scenario is more for one party to avoid, the other party will go straight ahead.

To address the above problem, this paper proposes a dynamic selection avoidance algorithm, which will decide whether to select avoidance based on the size of the mapping of the pedestrian's current velocity on the vector pointing to the opposite pedestrian. As shown in Figure 6, V_a and V_b are the actual velocities of entities A and B. V_a' is the mapping of V_a on vector AB, and V_b' is the mapping of V_b on vector BA. By comparing the relative magnitudes of V_a' and V_b' to choose to determine whether the pedestrians are avoiding or not.

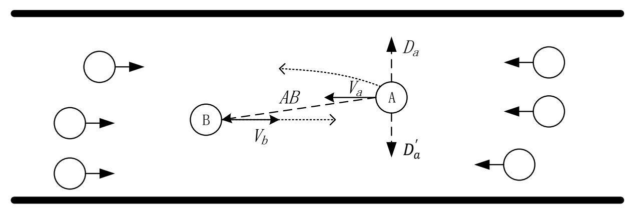

Fig. 6. Dynamic selection avoidance. Pedestrians will choose whether to evade according to the relative speed.

Judging whether pedestrians avoid is actually to judge whether there is a avoidance force. Based on obtaining the avoidance force in the dynamically selected direction, the improved avoidance force can be set to zero if no avoidance, and the improved avoidance force is defined as follows (4).

$$F_{imp} = A \cdot \exp(D/B) \cdot \cos\alpha \cdot D_a \cdot sign \tag{4}$$

Where Sign is a 0 or 1 function to determine the relative size of pedestrian A and B mapping speed, when $V_a' <= V_b'$,Sign returns to 1, otherwise 0, indicating that the pedestrian with a small speed is facing the oncoming pedestrian with a large speed, the pedestrian with a small speed to avoid, as expressed in equation (5).

$$sign = S\left(V_a' \leq V_b'?1 : 0\right) \tag{5}$$

Since the improved avoidance force needs to generate the complete trajectory, it requires three initial conditions: initial coordinates, initial velocity, and endpoint coordinates; the initial coordinates use the coordinates of the last frame of the observed trajectory; the initial velocity uses the higher-order velocity of the last two frames of the observed trajectory, i.e., the difference between the two coordinates; The endpoint coordinates are obtained by rotating sampling of the endpoint coordinates in the direction of pedestrian walking, The specific implementation is described in Section 3.1.In this algorithm, each pedestrian is regarded as a particle, and each particle follows Newton's second law of motion, so the resultant force F_{all} of pedestrian motion depends on the target attraction and the improved avoidance force. The target attractive force

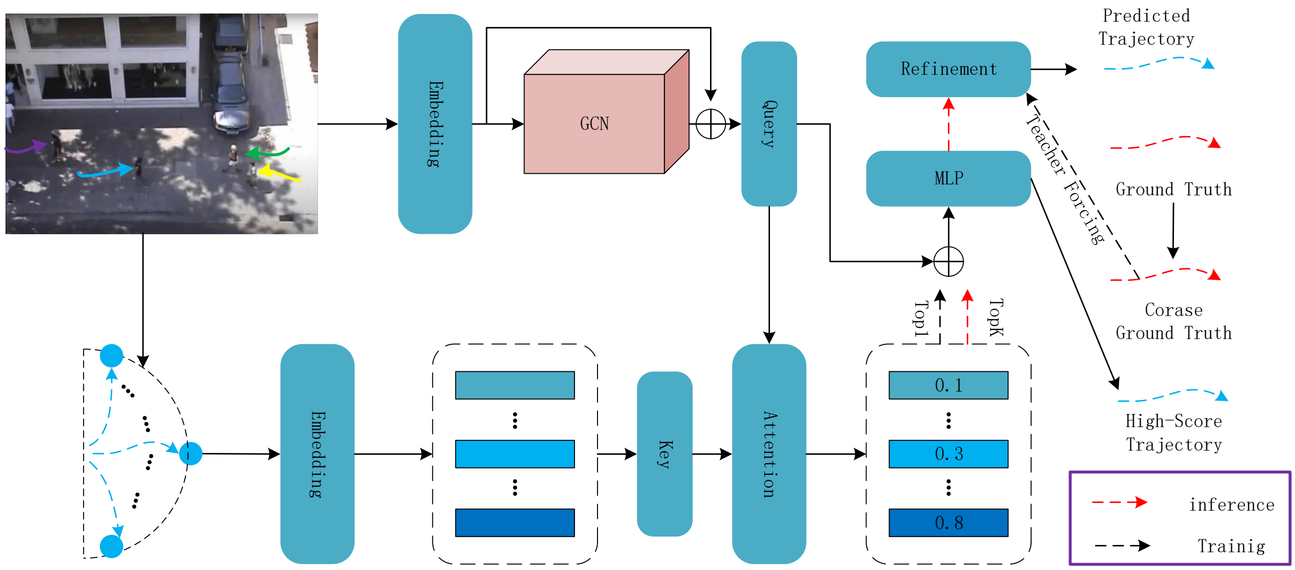

Fig. 7. model overview. The endpoint information of the pedestrian trajectory is generated using the observed trajectory, and the complete trajectory information is complemented by the improved avoidance force. Then, the generated improved avoidance force trajectories are embedded and encoded, while the spatial interactions of the observed trajectories are encoded, and by attention, each trajectory is scored, and the trajectories with high confidence are selected and optimized. Finally, the trajectories are further optimized using Teacher-forcing in the training process.

is defined in equation (6), and the combined force F_{all} is specifically expressed in equation (7).

$$F_{goal} = m\left(\left(V_0 \cdot \vec{e} - V\right)/t\right) \tag{6}$$

$$F_{all} = F_{goal} + \lambda F_{imp} \tag{7}$$

m is the pedestrian mass; V_0 is the desired velocity; V is the initial velocity; $\vec{e}$ is the direction vector of the pedestrian towards the destination; and t is the reaction time of the pedestrian; λ is the weight to improve avoidance force.

The trajectory of pedestrian is realized according to the speed and coordinates of the dynamic update of pedestrian, based on Newton's second law $F = ma$. The pedestrian is regarded as a particle, the pedestrian mass m is ignored, and a is the acceleration. Then the formula can be derived as $F = (V_{new} - v)/step$, and the updated velocity can be defined as Equation (8). Pedestrian coordinates are determined by pedestrian initial coordinates and displacement, and displacement is obtained by multiplying the current speed and time interval. Then the updated coordinates can be defined as Formula (9). The speed and coordinates are updated alternately, and all the coordinate points of future pedestrians are recurred, which is the pedestrian trajectory.

$$V_{new} = v + step \cdot F_{all} \tag{8}$$

$$P_{new} = p + step \cdot v \tag{9}$$

P is the initial coordinates of the pedestrian, i.e., the last frame of the observed trajectory, v is the initial velocity of the pedestrian, and $step$ is the time interval to update the next position.

IV. Trajectory Selection and Optimization

In order to select the best predicted trajectory from multiple improved avoidance force trajectories, the generated multiple trajectories need to be scored. Firstly, given the observation trajectory $X = \{x_i^t \mid t = 1, 2 \ldots, T_{obs}, i = 1, 2 \ldots, n\}$, the observation trajectory X and the avoidance force trajectory $Avoid_x$ are embedded and encoded by the embedding layer to obtain the observation code obs_e and the avoidance force trajectory code $Avoid_e$, respectively. The embedding layer $\psi()$ is realized by the three-layer MLP, which is represented as equations (10), (11).

$$obs_e = \psi(X) \tag{10}$$

$$Avoid_e = \psi\left(Avoid_x\right) \tag{11}$$

Pedestrian trajectory is not only related to the pedestrian's own motion state but also to the interaction of other pedestrians. Since self-attention can pay attention to each other's feature elements in the same group, the interaction features between pedestrians in the same group can be better captured. Therefore, the observation code obs_e is modeled by GCN implemented by self-attention to generate interactive code I_e. In order to select the trajectory with high confidence from multiple trajectories of improved collision avoidance force, the trajectory of collision avoidance force is coded $Avoid_e$ as the Key of attention, and I_e is coded intersely as the Query of attention, and the corresponding attention Score is obtained as the confidence score.which is represented as in equation (12).

$$Score = softmax\left(\psi\left(I_e\right)\phi\left(Avoid_e\right)^T\right) \tag{12}$$

In order to make the improved avoidance force trajectory closest to the ground truth value obtain the highest confidence, the path metric is used to measure the distance between each improved avoidance force trajectory and the true value, and the position in the improved avoidance force trajectory closest to the true value is used as the label $Score_{gt}$ to supervise the scoring operation, $Score_{gt}$ is obtained by measuring the ADE of the improved avoidance force trajectory and the true value. The loss function uses cross-entropy loss, and the specific loss function is as in equation (13).

$$Loss_{clf} = Loss_{ce}\left(Score, Score_{gt}\right) \tag{13}$$

In the training, in order to make the improved avoidance force trajectory $Avoid_s$ with the highest confidence better optimized, the interaction code I_e and $Avoid_s$ are fused into the MLP to obtain the predicted trajectory $Avoid_{pre}$, and the ground truth coarse trajectory $\hat{Y}$ is used for its supervised optimization. The loss function is Huber loss, and the specific optimized loss function is represented as in equation (14).

$$Loss_{reg} = Loss_{reg}\left(Avoid_{pre}, \hat{Y}\right) \tag{14}$$

The ground truth coarse trajectory $\hat{Y}$ is generated from the truth trajectory Y. First, the ground truth is divided into multiple equal-length segments with time interval S, and then the breakpoints are connected sequentially.

In order to make the trajectories with high confidence further refined to get more accurate prediction trajectories, Teacher-forcing is used for training, i.e., when Refinement is performed, the trajectory with the highest confidence score is replaced by the ground truth coarse trajectory $\hat{Y}$, and the final prediction trajectory $Avoid_f$ is obtained by Refinement refinement. i.e., optimization The loss function is as in Eq. (15), so the total loss of network training is as in Eq. (16).

$$Loss_{ref} = Loss_{reg}\left(Avoid_f, Y\right) \tag{15}$$

$$Loss = Loss_{ref} + Loss_{clf} + Loss_{reg} \tag{16}$$

Refinement consists of three layers of MLP; $Avoid_f$ is the final predicted trajectory output by the network, Y is the ground truth trajectory, and the loss function is Huber loss.In the inference, the top K predicted trajectories are selected according to the confidence scores, and the final prediction trajectories are obtained by Refinement refinement.

V. Experiments And Results

A. Datasets and evaluation criteria

The experiments are trained on two datasets for pedestrian trajectory prediction, ETH [23] and UCY [24]. ETH contains two scenarios, ETH and HOTEL, while UCY contains three scenarios, ZARA1, ZARA2 and UNIV. Trajectorys in the data set are sampled every 0.4 seconds. The data set contains 1536 trajectorys with rich interactive behaviors, including collision avoidance, deceleration avoidance, acceleration overtaking, etc.The training and evaluation follow the leave-one-out strategy[17],the model is trained on four scenes and evaluated on the rest of the scene.In the experimental parameter setting, the model observed trajectorys corresponding to 8 frames, 3.2 seconds, and predicted trajectorys for the next 4.8 seconds, namely 12 frames of pedestrian trajectorys.

The experimental evaluation criteria are evaluated using two metrics: Average Displacement Error (ADE) and Final Displacement Error (FDE). ADE measures the average L-2 distance between all predicted trajectory positions and the ground truth position. FDE measures the L-2 distance between the predicted position of the trajectory at the last moment and the true position.

B. Experimental parameter setting

In the experiment, the rotation angle of pedestrian endpoint sampling is set to $\pi/24$, and the cumulative angle of rotation sampling is less than $\pi/2$. The parameters related to the improved avoidance force and target attraction follow the settings of [4]. The weight m is set to 60KG; the force strength factor A is set to 1200N/m; the pedestrian force range is set to 0.3 m; the reaction time t of the pedestrian is set to 0.5 s; the desired velocity of the pedestrian is set to 1.3m/s. In the network, the number of dimensions of the embedding layers is set to 64 and the GCN cascade is set to 3 layers. In the inference stage, K=20 trajectories are selected as prediction trajectory.

C. Experimental result

The experimental results are shown in Table 1, and the experiments on the ETH and UCY datasets show that this algorithm outperforms the above algorithms, especially for the metric of FDE data. The algorithm in this paper improves 16% on the basis of Social-Implicit, and for the metric of ADE, the algorithm in this paper improves 6% on the basis of Social-Implicit. The analysis shows that the use of improved avoidance force can effectively capture the avoidance interaction information between pedestrians and therefore can obtain better prediction results.

D. Ablation study

To verify the influence of different avoidance strategies and different weight parameters on the overall prediction performance, ablation tests were conducted on the ETH and UCY datasets.

As shown in Table 2, the avoidance strategies contain dynamic directional decision avoidance and dynamic selection avoidance. The ablation experiments of avoidance strategies were carried out under the optimal weight of improved avoidance force .V1) Dynamic direction selection avoidance was removed and only pedestrians were allowed to avoid the right. The results show a 2% decrease in ADE and a 2% decrease in FDE, verifying the contribution of the dynamic direction selection avoidance algorithm to pedestrian trajectory prediction. V2) Remove dynamic direction selection avoidance, and pedestrians traveling in opposite directions both choose to avoid. The results show that ADE decreases by 7% and FDE decreases by 11%, especially for UNIV dataset, the performance decreases significantly. It is understood that UNIV is a university dataset, which is densely populated, and the situation of choosing to avoid is more common, and the situation of choosing to avoid both walking in opposite directions is less; therefore, the contribution of dynamic direction selection avoidance algorithm in this case is verified. The conclusions show that the removal of either component leads to a reduction in the accuracy of the prediction. The experimental results show that improving the avoidance force can effectively capture the avoidance patterns between pedestrians.

TABLE I
(ADE/FDE) EXPERIMENTS ON ETH AND UCY DATASETS.

Model	Year	ETH	HOTEL	UNIV	ZARA1	ZARA2	AVG
S-LSTM[2]	2016	1.09/2.35	0.79/1.76	0.67/1.40	0.47/1.00	0.56/1.17	0.72/1.54
SGAN[18]	2018	0.87/1.62	0.67/1.37	0.76/1.52	0.35/0.68	0.42/0.84	0.61/1.21
Sophie[14]	2019	0.70/1.43	0.76/1.67	0.54/1.24	0.30/0.63	0.38/0.78	0.51/1.15
S-BIGAT[15]	2019	0.69/1.29	0.49/1.01	0.55/1.32	0.30/0.62	0.36/0.75	0.48/1.00
GAT[15]	2019	0.68/1.29	0.68/1.40	0.57/1.29	0.29/0.60	0.37/0.75	0.52/1.07
SSTGCNN[19]	2020	0.64/1.11	0.49/0.85	0.44/0.79	0.34/0.53	0.30/0.48	0.44/0.75
STAR[16]	2020	0.56/1.11	0.26/0.50	0.52/1.15	0.41/0.90	0.31/0.71	0.41/0.87
SGCN[17]	2021	0.63/1.03	0.32/0.55	0.37/0.70	0.29/0.53	0.25/0.45	0.37/0.65
SImplicit[20]	2022	0.66/1.44	0.20/0.36	**0.31/0.60**	**0.25**/0.50	0.22/0.43	0.33/0.67
OURs	-	**0.41/0.72**	**0.17/0.30**	0.35/0.67	**0.25/0.47**	0.19/0.39	**0.27/0.51**

TABLE II
(ADE/FDE) ABLATION EXPERIMENT IN DIFFERENT COMPONENTS.

Model	ETH	HOTEL	UNIV	ZARA1	ZARA2	AVG
V1	0.44/**0.72**	0.18/0.33	0.37/0.71	**0.25**/0.49	0.22/0.42	0.29/0.53
V2	0.43/0.76	**0.17**/0.32	0.60/1.10	0.27/0.50	0.22/0.43	0.34/0.62
OURs	**0.41/0.72**	**0.17/0.30**	**0.35/0.67**	**0.25/0.47**	**0.19/0.39**	**0.27/0.51**

TABLE III
(ADE/FDE) DIFFERENT λ ABLATION EXPERIMENT OF WEIGHT IMPROVED AVOIDANCE.

Model	ETH	HOTEL	UNIV	ZARA1	ZARA2	AVG
($\lambda = 0.00$)	0.46/0.76	0.20/0.33	**0.34**/0.68	**0.25/0.47**	0.20/0.40	0.29/0.53
($\lambda = 0.25$)	0.44/0.75	0.20/0.34	0.36/0.72	**0.25**/0.48	0.20/0.42	0.29/0.54
($\lambda = 0.50$)	**0.41/0.72**	0.18/0.34	0.44/0.84	**0.25/0.47**	**0.19/0.39**	0.29/0.55
($\lambda = 0.75$)	0.43/0.74	0.18/0.31	0.49/0.91	**0.25**/0.48	0.20/0.42	0.31/0.57
($\lambda = 1.00$)	0.43/**0.72**	**0.17/0.30**	0.35/**0.67**	**0.25**/0.48	0.20/0.41	**0.28/0.52**

In order to verify the impact of different improved avoidance force weights on the prediction performance, this paper sets five different sizes of λ to find the appropriate weights, as shown in Table 3. $\lambda = 0$ means there is no avoidance effect between pedestrians; $\lambda = 0.5$ means there is some avoidance force between pedestrians; $\lambda = 1$ means pedestrians have a strong avoidance magnitude; the larger λ means the magnitude of pedestrian encounter avoidance is larger; the smaller λ means pedestrians the smaller magnitude of avoidance, or even no avoidance. The ablation study indicates that ETH, ZARA1, and ZARA2 perform optimally when $\lambda = 0.5$, and Hotel and UNIV perform optimally when $\lambda = 1$. Each dataset has the most suitable weight size applicable to itself.

E. *Visualization of results*

As shown in Figure 8, the visualization effects in the ETH and Hotel scenarios are displayed in the actual scenario. Bright yellow in the figure indicates the observation trajectory; Red represents the real trajectory; Green indicates the predicted trajectory; The blue color indicates the trajectory generated by the improved avoidance force. The twists and turns of the blue trajectory in the figure indicate the avoidance phenomenon when the improved avoidance force generates the trajectory; The figure can also accurately predict the standing pedestrian. It can be seen from the green prediction trajectory in the figure that the proposed algorithm can accurately predict the future trajectory of pedestrians.

VI. CONCLUSION AND FUTURE WORK

In this paper,We propose an improved collision avoidance algorithm to explicitly model the interaction between pedestrians and generate socially acceptable pedestrian trajectorys, which achieves good results with the ETH and UCY datasets. For the existing methods, the endpoint coordinate information is not accurately predicted, but the endpoint coordinate information is uniformly sampled, so there is still room for upward movement in the accuracy for trajectory prediction. In future work, how to fuse the observed trajectory information and scene map information to obtain accurate endpoint coordinate information is a direction worthy of research.

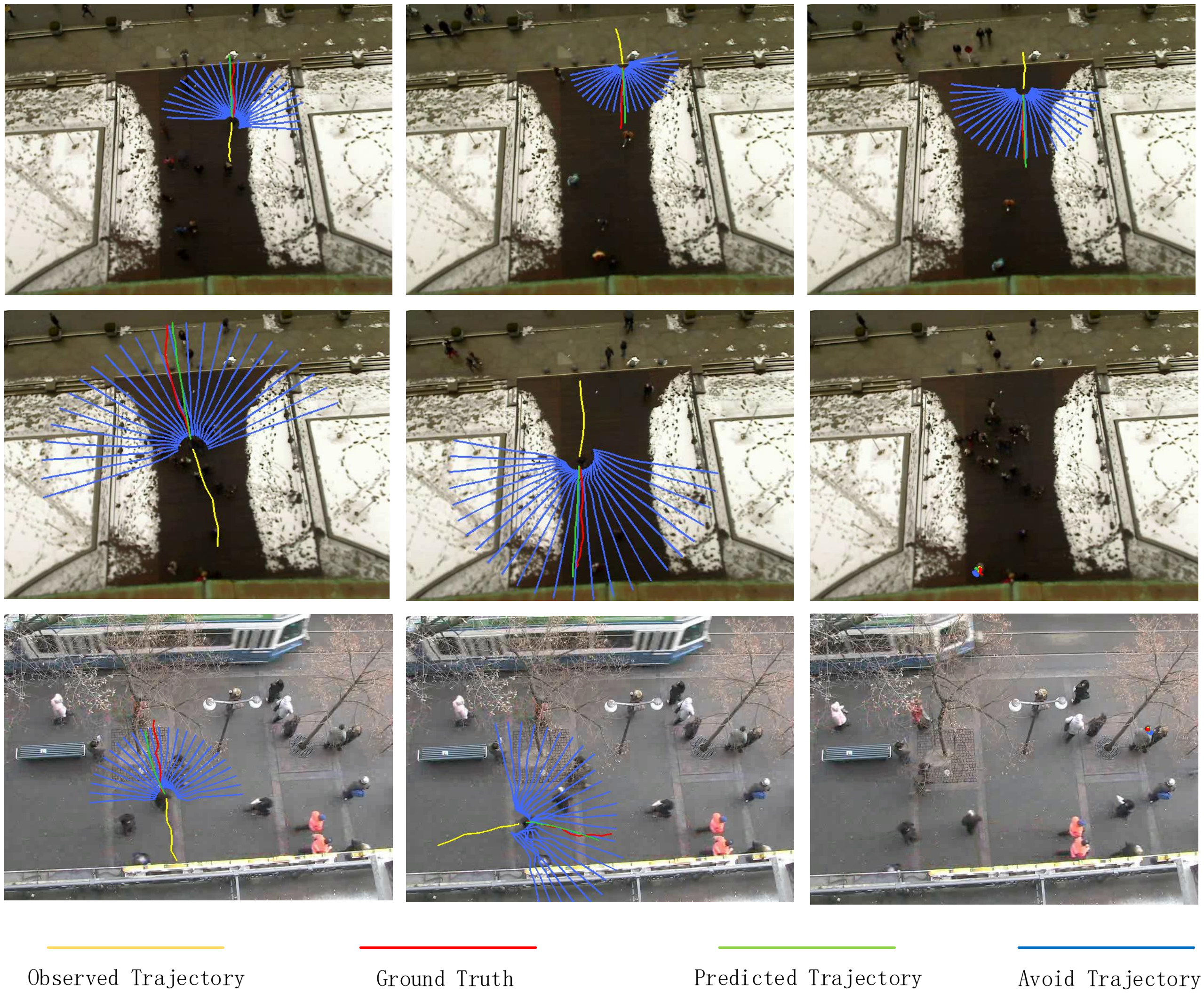

Fig. 8. Visualization representation. The graphs show the visualized trajectories in the ETH and UCY scenarios, respectively.

REFERENCES

[1] F. Large, D. Vasquez, T. Fraichard, and C. Laugier, "Avoiding cars and pedestrians using velocity obstacles and motion prediction," in *IEEE Intelligent Vehicles Symposium, 2004*. IEEE, 2004, pp. 375–379.

[2] A. Alahi, K. Goel, V. Ramanathan, A. Robicquet, L. Fei-Fei, and S. Savarese, "Social lstm: Human trajectory prediction in crowded spaces," in *Proceedings of the IEEE conference on computer vision and pattern recognition*, 2016, pp. 961–971.

[3] L. S. SHAN, Q. D. LIN, and W. J. ZHOU, "Improved social force model considering pedestrian deceleration and avoidance," *Journal of Jilin University: Engineering Edition*, vol. 42, no. 3, pp. 623–628, 2012.

[4] M. SHANG, Z. RUI, Q. Z. YANG, and H. J. TIAN, "A study on the improvement of the social force model of opposite direction pedestrian avoidance and contact behavior," *Computer Simulation*, vol. 38, no. 3, pp. 63–67, 2021.

[5] R. J. Williams, Zipser, and D, "a learning algorithm for continually running fully recurrent neural networks," 2017.

[6] D. Helbing and P. Molnar, "Social force model for pedestrian dynamics," *Physical review E*, vol. 51, no. 5, p. 4282, 1995.

[7] C. G. Keller and D. M. Gavrila, "Will the pedestrian cross? a study on pedestrian path prediction," *IEEE Transactions on Intelligent Transportation Systems*, vol. 15, no. 2, pp. 494–506, 2013.

[8] K. M. Kitani, B. D. Ziebart, J. A. Bagnell, and M. Hebert, "Activity forecasting," in *European conference on computer vision*. Springer, 2012, pp. 201–214.

[9] J. F. P. Kooij, N. Schneider, F. Flohr, and D. M. Gavrila, "Context-based pedestrian path prediction," in *European Conference on Computer Vision*. Springer, 2014, pp. 618–633.

[10] C. Long and G. Hua, "Correlational gaussian processes for cross-domain visual recognition," in *Proceedings of the IEEE Conference on Computer Vision and Pattern Recognition*, 2017, pp. 118–126.

[11] A. Islam, C. Long, and R. Radke, "A hybrid attention mechanism for weakly-supervised temporal action localization," in *Proceedings of the AAAI Conference on Artificial Intelligence*, vol. 35, no. 2, 2021, pp. 1637–1645.

[12] L. Dang, Y. Nie, C. Long, Q. Zhang, and G. Li, "Msr-gcn: Multi-scale residual graph convolution networks for human motion prediction," in *Proceedings of the IEEE/CVF International Conference on Computer Vision*, 2021, pp. 11 467–11 476.

[13] K. Xia, L. Wang, S. Zhou, G. Hua, and W. Tang, "Dual relation network for temporal action localization," *Pattern Recognition*, vol. 129, p. 108725, 2022.

[14] A. Sadeghian, V. Kosaraju, A. Sadeghian, N. Hirose, H. Rezatofighi, and S. Savarese, "Sophie: An attentive gan for predicting paths compliant to social and physical constraints," in *Proceedings of the IEEE/CVF conference on computer vision and pattern recognition*, 2019, pp. 1349–1358.

[15] V. Kosaraju, A. Sadeghian, R. Martín-Martín, I. Reid, H. Rezatofighi, and S. Savarese, "Social-bigat: Multimodal trajectory forecasting using bicycle-gan and graph attention networks," *Advances in Neural Information Processing Systems*, vol. 32, 2019.

[16] C. Yu, X. Ma, J. Ren, H. Zhao, and S. Yi, "Spatio-temporal graph

transformer networks for pedestrian trajectory prediction," in *European Conference on Computer Vision*. Springer, 2020, pp. 507–523.

[17] L. Shi, L. Wang, C. Long, S. Zhou, M. Zhou, Z. Niu, and G. Hua, "Sgcn: Sparse graph convolution network for pedestrian trajectory prediction," in *Proceedings of the IEEE/CVF Conference on Computer Vision and Pattern Recognition*, 2021, pp. 8994–9003.

[18] A. Gupta, J. Johnson, L. Fei-Fei, S. Savarese, and A. Alahi, "Social gan: Socially acceptable trajectories with generative adversarial networks," in *Proceedings of the IEEE conference on computer vision and pattern recognition*, 2018, pp. 2255–2264.

[19] A. Mohamed, K. Qian, M. Elhoseiny, and C. Claudel, "Social-stgcnn: A social spatio-temporal graph convolutional neural network for human trajectory prediction," in *Proceedings of the IEEE/CVF Conference on Computer Vision and Pattern Recognition*, 2020, pp. 14 424–14 432.

[20] A. Mohamed, D. Zhu, W. Vu, M. Elhoseiny, and C. Claudel, "Social-implicit: Rethinking trajectory prediction evaluation and the effectiveness of implicit maximum likelihood estimation," *arXiv preprint arXiv:2203.03057*, 2022.

[21] T. N. Kipf and M. Welling, "Semi-supervised classification with graph convolutional networks," *arXiv preprint arXiv:1609.02907*, 2016.

[22] A. Vaswani, N. Shazeer, N. Parmar, J. Uszkoreit, L. Jones, A. N. Gomez, Ł. Kaiser, and I. Polosukhin, "Attention is all you need," *Advances in neural information processing systems*, vol. 30, 2017.

[23] S. Pellegrini, A. Ess, K. Schindler, and L. Van Gool, "You'll never walk alone: Modeling social behavior for multi-target tracking," in *2009 IEEE 12th international conference on computer vision*. IEEE, 2009, pp. 261–268.

[24] A. Lerner, Y. Chrysanthou, and D. Lischinski, "Crowds by example," in *Computer graphics forum*, vol. 26, no. 3. Wiley Online Library, 2007, pp. 655–664.